Biological Forum – An International Journal **15(6): 1035-1046(2023)**

ISSN No. (Print): 0975-1130
ISSN No. (Online): 2249-3239

Formulation, Development and Characterization of Microsponges of Flutrimazole

Yogesh Kumar Garg[1*] and Amit Bhargava[2]
[1]Reserach Scholar, Faculty of Pharmacy, Bhupal Nobles' University, Udaipur (Rajasthan), India.
[2]Assistant Professor, Faculty of Pharmacy, Bhupal Nobles' University, Udaipur (Rajasthan), India.

(Corresponding author: Yogesh Kumar Garg)*
(Received: 13 April 2023; Revised: 15 May 2023; Accepted: 23 May 2023; Published: 15 June 2023)
(Published by Research Trend)

ABSTRACT: Flutrimazole, recognized for its broad-spectrum antifungal properties, encounters challenges including low solubility and restricted skin penetration, which ultimately impact its therapeutic effectiveness. This study aims to address these challenges by concentrating on the formulation, development, and characterization of microsponges that encapsulate Flutrimazole, thereby enhancing drug delivery efficacy. The microsponges were synthesized through a quasi-emulsion solvent diffusion technique, with optimization focused on various parameters including particle size, drug entrapment efficiency, surface morphology, and in vitro drug release profiles. The formulations that were meticulously prepared underwent evaluation through scanning electron microscopy (SEM) to analyze their structure, differential scanning calorimetry (DSC) to investigate their thermal properties, and Fourier-transform infrared spectroscopy (FTIR) to examine the chemical interactions present. The in vitro drug release investigations revealed a meticulously regulated and prolonged release pattern, indicating improved permeation and retention within the layers of the skin.

Keywords: Flutrimazole, Antifungal, Microsponges, Gel, Formulation.

INTRODUCTION

Topical drug delivery systems have gained substantial attention owing to their capability to provide localized drug action with minimal systemic absorption (Singh *et al*., 2016; Ranade, 1991). Among various topical drug delivery approaches, microsponge-based drug delivery systems have appeared as a promising technology for enhancing the therapeutic efficacy of antifungal agents like Flutrimazole (Raina *et al*., 2023). Flutrimazole, an imidazole-class antifungal agent, is widely used for treating superficial fungal infections. However, its conventional formulations often face challenges such as low skin retention, poor penetration, and undesirable side effects like irritation and burning sensation (Koparde *et al*., 2023; Nafisi and Maibach 2018; Prashanth *et al*., 2022).

Microsponges, as a controlled drug delivery system, offer several advantages, including sustained drug release, enhanced stability, reduced side effects, and improved patient compliance (Kaity *et al*., 2010; Aloorkar *et al*., 2012). These porous, polymeric microspheres can encapsulate active pharmaceutical ingredients (APIs) and facilitate their controlled diffusion, ensuring prolonged action at the site of infection (Lengyel *et al*., 2019; Nevle & Butle 2023). This property is particularly beneficial for antifungal treatments, where maintaining an optimal drug concentration over an extended period is crucial for effective therapy (Lewis, 2011).

The development of Flutrimazole-loaded microsponges involves the selection of appropriate polymers, optimization of formulation parameters, and thorough physicochemical characterization to ensure efficacy and stability (Merlos *et al*., 1996; Alomar *et al*., 1995). Key characterization techniques include particle size analysis, drug entrapment efficiency, surface morphology, in vitro drug release studies, and ex vivo skin permeation studies. By incorporating microsponges into a topical formulation, the therapeutic efficiency of Flutrimazole can be significantly improved while minimizing adverse effects (Bargal *et al*., 2013; Syed *et al*., 2020; Thakur & Desai 2023).

This study aims to formulate, develop, and characterize microsponges of Flutrimazole, optimizing their properties for effective topical antifungal therapy. The research focuses on evaluating the impact of formulation variables on drug loading, release kinetics, and stability to establish a novel, patient-friendly delivery system for treating fungal infections.

MATERIAL AND METHODS

Procurement of Drug . The drug Flumitrazole was received as gifted sample from FDC Limited, Raigad.

Preformulation Studies. The drugs were tested for organoleptic properties such as appearance, colour, taste, etc.

Melting Point Determination. The melting point of the drugs was determined by melting point apparatus.

Solubility Analysis. Preformulation solubility analysis was done to select a suitable solvent system to dissolve

the drug and also to test its solubility in the dissolution medium, to be used.

UV spectroscopy: (Determination of λ_{max}). The stock solutions of the drugs, at a concentration of 100µg/mL, were meticulously prepared using methanol as the solvent for Flutrimazole. The stock solutions were meticulously diluted using the corresponding solvents to achieve a concentration of 20µg/mL. The ultraviolet spectrum was meticulously documented within the range of 200-400 nm utilizing a Schimadzu 1700 UV spectrophotometer to ascertain the λmax.

IR Spectroscopy. The spectrum was captured within the wavelength range of 4000 to 400 cm-1. A dry sample of the drug, along with potassium bromide, was meticulously blended and placed into the die cavity of the sample holder, followed by the recording of an IR spectrum utilizing a diffuse reflectance FTIR spectrophotometer.

Construction of Calibration Curve for Drugs. A stock solution with a concentration of 100 µg/mL was meticulously prepared by dissolving 10 mg of Flutrimazole in methanol within a 100 mL volumetric flask. From the stock solution, a series of solutions were meticulously prepared, containing 2, 4, 6, 8, 10, 12, 14, 16, 18, and 20 µg/mL of the drugs through precise dilutions. The absorbance of these solutions was recorded at 296 nm for Salicylic acid and at 238 nm for Flutrimazole, using their respective blank solvents as references.

Drug-Excipient Compatibility Studies. Compatibility studies between drug and excipients were conducted over a duration of one month. The formulation containing excipients Eudragit RS 100 and PVA was placed under storage conditions at room temperature as well as at an elevated temperature of 45°C with 75% relative humidity in a stability chamber for a duration of one month. Samples were collected after 7, 14, 21, and 30 days to assess the subsequent parameter.

Physical change. The samples underwent examination for physical alterations, including discoloration and odor, among other factors.

FTIR study. The anhydrous mixture of the drug and potassium bromide was meticulously blended and subsequently placed into the die cavity of the sample holder, followed by the acquisition of an IR spectrum utilizing a diffuse reflectance **FTIR spectrophotometer.**

Formulation Development of microsponges

Free Radical Polymerization Reactions: Fundamentals

Addition polymers can indeed be synthesized from monomers that feature C=C double bonds; a significant number of these compounds undergo spontaneous polymerization unless measures are taken to inhibit the process. To initiate the polymerization reaction resulting in an addition polymer, one can effectively introduce a free radical source to the monomer. The concept of a free radical refers to a group of highly reactive and transient entities within a chemical reaction, characterized by the presence of one or more unpaired electrons. In the context of free radicals, addition polymers emerge through a dynamic chain reaction mechanism, encompassing stages of chain initiation, chain propagation, and chain termination.

Chain initiation

To commence the chain reaction, it is essential to have a source of free radicals. Free radicals are typically generated through the decomposition of peroxides, such as di-tert-butyl peroxide or benzoyl peroxide, as illustrated below. When exposed to heat or light, peroxides undergo decomposition, resulting in the formation of a duo of free radicals characterized by an unpaired electron.

Chain propagation. In the initial phase of the chain reaction, a free radical emerges and subsequently interacts with an alkene, resulting in the formation of a novel free radical. The outcome of this reaction can subsequently incorporate further monomers in a sequential process.

Chain termination. When pairs of radicals unite to create a covalent bond, the chain reactions facilitated by these radicals come to a halt.

The formation of branched polymers. It is reasonable to anticipate that the outcome of the free radical polymerization of ethylene will yield a linear chain polymer. As the chain expands, it starts to curve back upon itself. This facilitates an intra-molecular reaction wherein the locus of polymerization shifts from the terminal end of the chain to a carbon atom situated along the backbone.

At this juncture, branches are incorporated into the polymer chain. The process of free radical polymerization of ethylene yields a polymer characterized by the presence of branches, which constitute between 1% and 5% of the total carbon atoms. Among these branches, 10% consist of two carbon atoms, 50% comprise four carbon atoms, and 40% are characterized by longer side chains.

Preparation of Flutrimazole Microsponges by Liquid-liquid Suspension Polymerization method. Flutrimazole exhibited sensitivity to the reaction conditions inherent in suspension polymerization techniques. Consequently, the quasi-emulsion solvent diffusion method was selected for the preparation of Eudragit-based microsponges.

Quasi-emulsion Solvent Diffusion method: (Eudragit microsponges). In the preparation of the inner phase, Eudragit RS 100 was solubilized in 3 mL of methanol, followed by the incorporation of triethylcitrate (TEC) at a concentration of 20% relative to the polymer to enhance plasticity. The drug is subsequently incorporated into this solution and dissolved through the process of ultrasonication at a temperature of 35°C. The inner phase was introduced into the PVA (72000) solution within 200 mL of water, constituting the outer phase. The resulting mixture underwent stirring for a duration of 60 minutes, followed by filtration to isolate the microsponges. The microsponges underwent a washing and drying process at a temperature of 40°C for a duration of 24 hours.

Seven distinct ratios of drug to Eudragit RS 100 (1:1, 3:1, 5:1, 7:1, 9:1, 11:1, and 13:1) were utilized to investigate the influence of the drug-polymer ratio on the physical characteristics and dissolution properties of

microsponges. The agitation speed utilized was 500 rpm, employing three-blade propeller stirrers.

Table 1: Microsponge formulations using Eudragit RS100.

Constituents	Flutrimazole Microsponges						
	F1	F2	F3	F4	F5	F6	F7
Inner phase							
Flutrimazole	2.5	2.5	2.5	2.5	2.5	2.5	2.5
Eudragit RS 100 (g)	2.5	0.83	0.50	0.36	0.28	0.23	0.19
Methanol (mL)	3	3	3	3	3	3	3
Outer phase							
Distilled water (mL)	200	200	200	200	200	200	200
PVA 72000 (mg)	50	50	50	50	50	50	50

Evaluation of Microsponges. Determination of Production Yield and Loading Efficiency

The yield of the micro particles was ascertained through a precise calculation of the initial weight of the raw materials in conjunction with the final weight of the resulting microsponge.

$$\text{Production Yield} = \frac{\text{Practical Mass of Microsponges}}{\text{Theoretical Mass (Polymer + drug)}} \times 100$$

The efficiency of loading (%) for the microsponges can be determined using the subsequent equation:

$$\text{Loading Efficency} = \frac{\text{Actual Drug Content in Microsponges}}{\text{Theoretical drug Content}} \times 100$$

Particle Size Analysis. The analysis of particle size for the prepared microsponges was conducted utilizing the Malvern Particle Size Analyzer Hydro 2000 MU (A). Microsponges were suspended in double distilled water prior to conducting the sample analysis in the instrument, ensuring that the light scattering signal, as reflected by the particle count per second, remained within the instrument's sensitivity range. This system is characterized by its flexibility, modular design, and complete integration, ensuring reliable measurement performance across a range from submicron to millimeter sizes. This method is capable of quantifying the particle size of both wet and dry substances, utilizing milligram amounts of valuable pharmaceuticals.

In the course of the measurement, particles traverse a concentrated laser beam. The scattering of light by these particles occurs at an angle that is inversely related to their size. The angular intensity of the scattered light is subsequently assessed through a collection of photosensitive detectors. The graphical representation of scattering intensity in relation to angle serves as the fundamental basis for determining particle size. The Mie scattering model provides precise predictions regarding the scattering of particles. The Mastersizer 2000 software facilitates precise sizing across an extensive dynamic range.

Scanning Electron Microscopy. To investigate morphology and surface topography, microsponges were meticulously coated with platinum at room temperature, enabling a detailed examination of their surface morphology through scanning electron microscopy (SEM). The Scanning Electron Microscope (SEM), belonging to the same family of imaging technologies, stands as the most prevalent among all electron beam instruments. The Scanning Electron Microscope (SEM) utilizes a concentrated beam of electrons, generally ranging from several hundred electron volts to approximately 30 kiloelectron volts, which is systematically directed across the surface of a sample in a rectangular scanning pattern. Signals produced during electron irradiation are gathered, enhanced, and subsequently employed to adjust the luminosity of an appropriate display device, which is scanned in harmony with the probe beam.

Infrared Spectroscopy. The analysis was performed utilizing the Perkin Elmer, Spectrum 100 FT-IR spectrometer through FTIR spectroscopy. The spectrum was captured within the wavelength range of 4000 to 400 cm^{-1}. The procedure involved the careful dispersion of a sample in an excess of potassium bromide, adhering to a nearly 1:100 ratio. The components were thoroughly mixed, and the resulting mixture was subsequently placed into the sample holder for analysis.

Differential Scanning Calorimetry (DSC). The powder sample of microsponges was hermetically kept in the aluminum pan and heated at constant rate 5°C/min, over temperature range of 10°C to 250°C. An inert atmosphere was maintained by purging nitrogen at the flow rate of 100 mL/min.

Powder X-ray Diffraction Studies. In order to ascertain the physical state of the drug in its pure form and to examine the alterations in the crystallinity of the formulation components, a PXRD study was conducted utilizing an X-ray diffractometer. A voltage of 40 kV and a current of 40 mA were applied to the generator, utilizing copper as the anode material for the tube. The analysis of the pure drug samples and the microsponge formulation was conducted within the angular range of 5° to 50° (2θ).

Characterization of Pore Structure. The characterization of powders and solid materials is predominantly achieved through the application of physical and chemical gas adsorption techniques, alongside mercury intrusion porosimetry (MIP), which are recognized as the most prevalent methodologies in this field. The determination of pore diameter range, specifically between 0.3 and 300 nm, encompassing mesopores and macropores, is achieved through nitrogen gas adsorption, contingent upon the equipment employed. Low-pressure mercury porosimetry is employed to ascertain the presence of macropores, characterized by a pore diameter ranging from 14 to 200 µm. Conversely, high-pressure porosimetry facilitates the analysis of both mesopores and macropores, with pore diameters extending from 3 nm to 14 µm, contingent upon the specific equipment utilized. Both techniques offer dependable insights into the distribution of pore size and volume, particle size, bulk density, and specific surface area for porous solids, irrespective of their characteristics and form. Nonetheless, the relevant pore size ranges for each technique exhibit distinct variations.

Gas sorption and mercury porosimetry may serve as complementary methodologies. Techniques of

physical adsorption have the capacity to extend the lower limit of size measurement to approximately 0.00035 mm in diameter, thereby allowing for an exploration of the microstructure within particles. Mercury porosimetry is combined with the gas sorption technique to acquire porosity data across a broad size spectrum (exceeding approximately 0.3 mm in diameter and reaching up to around 360 mm), a range that gas sorption alone cannot achieve. When employing two distinct techniques, it is not prudent to anticipate identical outcomes within the overlapping or shared range of both instruments. Nonetheless, similar findings have been documented for certain materials.

Mercury intrusion porosimetry (MIP). The porosity parameters of microsponges, including intrusion–extrusion isotherms, pore size distribution, total pore surface area, average pore diameters, as well as the shape and morphology of the pores, along with bulk and apparent density, can be assessed through the application of mercury intrusion porosimetry. Incremental intrusion volumes may be graphically represented in relation to pore diameters, illustrating the distributions of pore sizes. The diameter of pores within microsponges can be determined through the application of the Washburn equation.

The characterization of pore morphology was conducted through the analysis of the intrusion–extrusion profiles of mercury within the microsponges, as outlined by Orr.

An ordinary MIP test consists of introducing a sample into a designated container, followed by the evacuation of the container to eliminate contaminant gases and vapors, predominantly water. While the container remains evacuated, mercury is permitted to fill the space within. This establishes a setting that includes a solid, a non-wetting liquid (mercury), and the vapor of mercury. Subsequently, the pressure is elevated to match the ambient conditions, while the influx of mercury into the larger apertures of the sample bulk is carefully observed. Upon the return of pressure to ambient levels, pores with diameters as small as approximately 12 mm have been completely filled. The sample container is subsequently positioned within a pressure vessel for the duration of the test. A typical maximum pressure of approximately 60,000 psia (414 MPa) is observed in commercial instruments, which enables the penetration of mercury into pores as small as 0.003 mm in diameter. The quantity of mercury that permeates the sample as a result of a pressure elevation from Pi to Pi+1 corresponds precisely to the volume of the pores within the specified size interval from ri to ri+1, with the dimensions being ascertained by applying the pressure values into Washburn's equation.

The measurement of the volume of mercury moving into the sample may be accomplished in various ways. Nonetheless, electronic methods for detecting the fluctuations of mercury within the capillary exhibit significantly enhanced sensitivity, achieving remarkable volume sensitivity to levels below a microliter. The collection of a sequence of applied pressures alongside the total volumes of mercury that have been intruded at each respective pressure forms the foundational data set. The graphical representation of this data is referred to as the intrusion curve. Upon the reduction of pressure, mercury is expelled from the pores, or it extrudes. The graphical representation of this data is referred to as the extrusion curve. The configuration of the pores and various physical phenomena typically results in the extrusion curve not adhering to the same trajectory as the intrusion curve when plotted. The intrusion and extrusion curve gives information about the pore network. The sample cup is equipped with a capillary stem, which functions dually as the mercury reservoir throughout the analysis and as a component of the mercury volume transducer. Before commencing each analysis, the sample cup and capillary are infused with mercury. Upon completion of the filling process, the primary source of mercury is eliminated, resulting in the retention of mercury solely within the sample cup and capillary stem, collectively designated as the penetrometer. Pressure is exerted on the mercury within the capillary through the influence of a gas, such as air, or a liquid, such as oil. The force is conveyed from the distant extremity of the capillary to the mercury enveloping the specimen within the sample cup. The capillary stem is constructed of glass (an electrical insulator), is filled with mercury (an electrical conductor), and the outer surface of the capillary stem is plated with metal (an electrical conductor). The arrangement of two concentric electrical conductors, with an insulating layer in between, results in the formation of a co-axial capacitor. The value of the capacitance is a function of the areas of the conductors, the dielectric constant of the insulator, and other physical parameters. In the case of this particular capacitor, the only variable is the area of the interior conductor as mercury leaves the capillary and enters the sample voids and pores, or as it moves back into the capillary when pressure is reduced. This is mechanically analogous to a mercury thermometer in which case mercury moves in and out of a calibrated capillary from a large bulb at one end. A small volume of mercury entering or leaving a small capillary causes the length (and area) of the mercury column to change significantly, thus providing volume-measuring sensitivity and resolution. In the case of the thermometer, the change in volume is proportional to the change in temperature by the coefficient of volumetric expansion of mercury. The capacitance value of the stem is monitored by a capacitance detector that, similar to the pressure transducer electronics, produces an electrical signal that is proportional to capacitance. Capacitance measurements are transformed into volume measurements by knowledge of the diameter of the precision capillary and the equation governing coaxial capacitors.

BET (Nitrogen adsorption) method. The AUTOSORB-1C analyzer, developed by

Quantachrome in the USA, operates under microprocessor control and is compatible with a PC running Windows 95, 98, or 2000. It employs Quantachrome's advanced software for data acquisition and reduction.

Surface area and pore size of the particles were determined using following methods:

- Adsorption and desorption isotherms.
- Multi and single point BET surface area (including C constant and correlation coefficient).
- Mesopore volume and area distribution (BJH and DH methods).

A vacant sample cell was weighed, followed by the addition of 0.043 g of the sample, after which quartz wool was inserted into it. The sample underwent activation at a temperature of 115°C for a duration of 12 hours, utilizing Nitrogen as the adsorbate. Following a duration of 12 hours, the sample cell was extracted from the activation station, allowed to cool to room temperature, and subsequently weighed once more. The final weight was determined by subtracting the weight of the sample cell, resulting in an exact sample weight of 0.04 g. The sample was subsequently positioned at the analysis station, and the examination commenced at the frigid temperature of liquid nitrogen (-196°C). Throughout the comprehensive analysis, the P/Po tolerance was upheld at three, while the equilibrium time was consistently set at two. Throughout the analysis, the system underwent a purging process utilizing helium. The data collected underwent analysis through the suitable software, Autosorb for Windows version 1.24.

***In-vitro* Release Study of Microsponges.** Precisely measured microsponges, each weighing 5mg, were introduced into 50 ml of an ethanol/methanol solution within 100 ml glass containers. The samples were subjected to horizontal shaking at 37°C at specified time intervals. Appropriate samples were extracted and substituted with fresh medium, subsequently analyzed using UV spectrophotometry at a wavelength of 238 nm for the detection of Flutrimazole. The concentrations of the drugs were assessed at various time intervals extending up to 6 hours.

Stability Profile of Microsponge Formulation. The aim of stability testing is to furnish evidence regarding the fluctuations in quality of an active substance or pharmaceutical product over time, influenced by a range of environmental factors including temperature, humidity, and light. The stability of the active component serves as the primary criterion in the rationale design and evaluation of dosage forms for drugs, ultimately influencing their acceptance or rejection. Throughout the stability studies, the product undergoes exposure to typical conditions of temperature and humidity. Nevertheless, the research requires an extended duration, making it advantageous to conduct accelerated stability studies in which the product is subjected to extreme temperature conditions. In order to evaluate the stability of the drug and formulation, stability studies were conducted in accordance with the guidelines set forth by ICH and WHO. The formulation was meticulously optimized and sealed within aluminum packaging, which featured an interior coating of polyethylene. Multiple replicates were stored in a humidity chamber, carefully regulated at 40±2°C and 75±5% RH for a duration of six months. The samples underwent analysis to assess the physical changes and in-vitro release profile at intervals of one month and six months.

Formulation of gel loaded with microsponges and plain drug

Table 2: Composition of gels.

Ingredients	Quantity (% w/w)
Drug (free or entrapped, equivalent to)	Flutrimazole : 2
Propylene glycol	40
Methanol	8
Menthol	0.04
Methyl paraben	0.18
Sodium meta bisulphite	0.10
Disodium edentate	0.10
Carbopol 934	1.00
Tri ethanolamine	q. s.
Purified water q. s. to make	100

A well-defined dispersion of carbopol was formulated in water through the application of moderate agitation. The intermittent addition of carbopol effectively mitigates the formation of lumps, leading to a clear and homogeneous dispersion. The formulation containing the drug or drug-loaded microsponges was dispersed in a mixture of propylene glycol and methanol. A variety of ingredients, including paraben, sodium meta bisulphite, and disodium edetate, were dissolved in water and subsequently incorporated into the drug solvent system. Triethanolamine was employed for neutralization and subsequently adjusted to the final weight with water. The gels that were prepared underwent a process of degassing through ultrasonication.

Evaluation of gel loaded with microsponges and plain drug

Determination of Viscosity. Viscosity of the formulated gels was determined by Brookfield Viscometer using Spindle type 93/T-C.

Drug Diffusion from Microspongic Gels. The in-vitro assessment of drug permeation across a cellophane membrane was conducted utilizing a Franz Diffusion cell. One gram of gels, either containing free or entrapped drug, was positioned in the donor compartment, whereas the receptor compartment held 12 mL of the receptor phase. At appropriate intervals, aliquots of 0.5 mL samples were extracted from the receptor compartment, and the drug was analyzed using spectrophotometric methods.

RESULTS AND DISCUSSION

Characterization of Flutrimazole Pure Drug

Table 3: Characterization of Flutrimazole Pure Drug.

Sr. No.	Characters	Specification	Result
1.	Description	White or almost white powder., crystalline powder	White or almost white powder., crystalline powder
2.	Melting point	161-166°C	161-166°C
3.	Solubility	insoluble in water, freely soluble in tetrahydrofuran, soluble in methanol..	insoluble in water, freely soluble in tetrahydrofuran, soluble in methanol.

Spectroscopic Studies

UV Spectroscopy:(Determination of λ_{max})

The UV spectrum of Flutrimazole in methanol was analyzed, revealing a λ_{max} of 256 nm.

IR Spectroscopy: The IR spectra of Flutrimazole in their pure form were meticulously recorded. The findings are illustrated in Table 4.

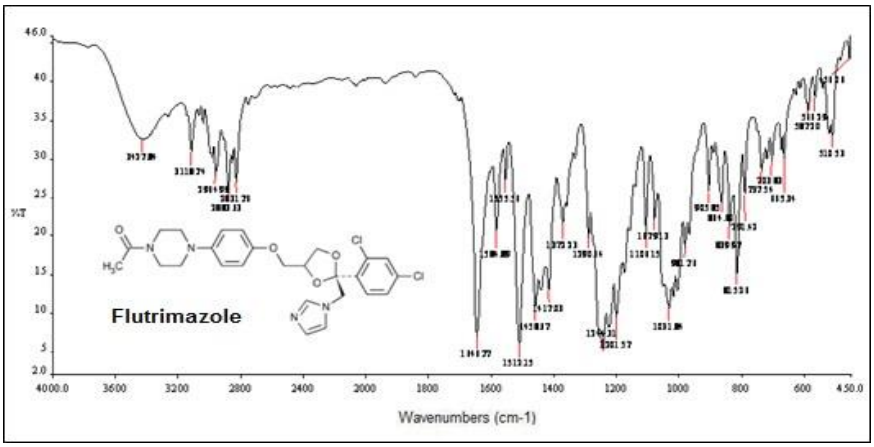

Fig. 1. IR Spectra of Flutrimazole.

Table 4: IR Spectrum interpretation of Flutrimazole.

Functional group	Wave number observed(cm^{-1})
C=O (carbonyl group)	1646.77
C-O (aliphatic ether group)	1031.84
C-O (cyclicether)	1244.31

Calibration curve of Flutrimazole

Table 5: Calibration curve data for Flutrimazole.

Sr. No.	Concentration (µg/mL)	Absorbance at 256 nm*
1.	2	0.055± 0.0031
2.	4	0.08±0.0025
3.	6	0.127±0.0024
4.	8	0.175±0.0012
5.	10	0.194±0.0036
6.	12	0.232±0.0014
7.	14	0.262±0.0047
8.	16	0.301±0.0024
9.	18	0.332±0.0071
10.	20	0.36±0.0031

*Each value is average of three separate determinations ±SD

Drug-excipient Compatibility Studies

Physical Change. No physical alterations, including changes in texture, or discoloration were noted throughout the compatibility study.

FTIR Study. The FTIR spectra of the three 'pure drugs' and the 'drug entrapped microsponges' were analyzed to investigate the potential incompatibility between the drugs and the excipients, as well as the effects of the reaction conditions. The principal peaks of microsponge-entrapped drugs were analyzed in relation to the peaks of pure drugs to determine their concordance. Fig. 2 presents an overlay of FTIR spectra for both pure and entrapped drugs.

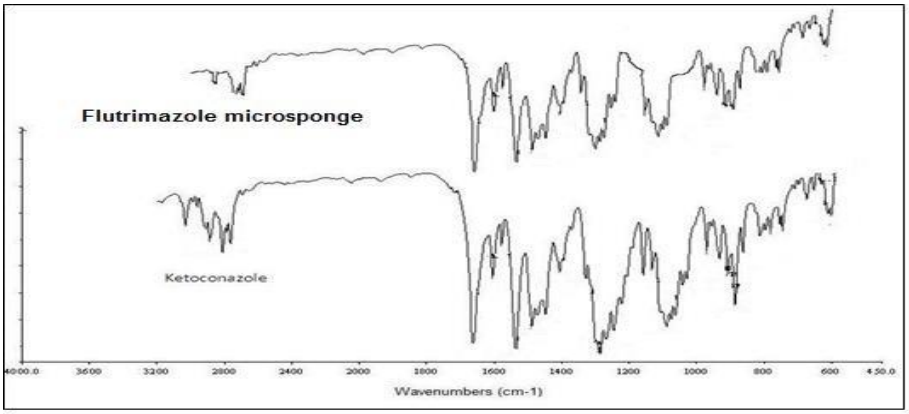

Fig. 2. Compatibility study of Flutrimazole by IR.

The principal peaks of the drugs were seen to be retained; the broadening of these peaks may be attributed to the overlap between the peaks of the polymer system and the medication within the microsponge formulation.

Evaluation of Microsponges

Production Yield

Table 6: Production yield of Flutrimazole microsponge.

Formulation code	Production yield(%)
F1	77.19±2.13
F2	80.23±1.17
F3	82.21±1.23
F4	85.12±2.01
F5	87.25±1.14
F6	89.14±1.90
F7	90.17±2.16

*****Each value is average of three separate determinations ±SD

The production yield of Flutrimazole microsponges ranged from 77.19% to 90.17% as illustrated in Table 6. The investigation into Eudragit RS 100 microsponges demonstrated that an increase in the drug to polymer ratio correlates with a rise in the production yield of the microsponges.

Drug Loading Efficiency. Table 7 presents the efficiencies of medication loading for Flutrimazole microsponges. The loading effectiveness observed in Flutrimazole microsponges was notably high, ranging from 85.36% to 94.89%. For Eudragit RS 100 microsponges, a boost in the medication to polymer proportion correlates with a rise in medication loading effectiveness.

Table 7: Drug loading efficiency of Flutrimazole microsponge formulations.

Formulation code	Drug Loading efficiency (%)
F1	85.36±1.32
F2	86.45±0.69
F3	88.49±2.01
F4	90.86±0.27
F5	92.38±1.26
F6	94.21±0.39
F7	94.89±0.16

*****Each value is average of three separate determinations ±SD

Scanning Electron Microscopy. The morphology of the microsponges, crafted through the trapping technique and the quasi-emulsion solvent diffusion approach, was examined using scanning electron microscopy (SEM) (Chen *et al.*, 2020). Fig. 3 presents some representative SEM images of the microsponges. SEM images demonstrated that the microsponges synthesized through the liquid-liquid suspension polymerization method (Flutrimazole microsponge) exhibited a finely spherical and uniform morphology. A closer examination of a microsponge unveiled the distinctive internal pores present on its surfaces. Eudragit RS 100 microsponges were synthesized utilizing the quasi-emulsion solvent diffusion technique.

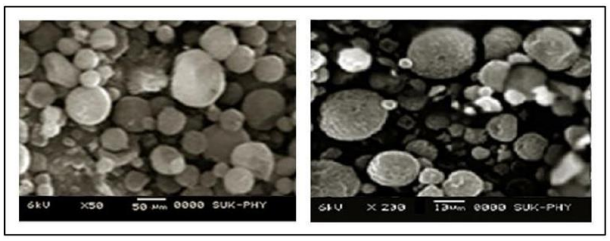

Fig. 3. SEM Photographs of Flutrimazole microsponges.

Particle Size Analysis. By meticulously regulating particle size throughout the polymerization processes, one can achieve free-flowing powders that exhibit refined aesthetic qualities. Representative of the particle size distribution of Eudragit based microsponges (Flutrimazole microsponge) are shown in Fig. 4. Mean particle size Flutrimazole was found to be 12.06 µm.

Infrared Spectroscopy. FTIR spectra of Flutrimazole, Eudragit RS 100 and microsponges formulated by Eudragit approach (F7) and overlay spectra are, as shown in Fig. 5-8 respectively.

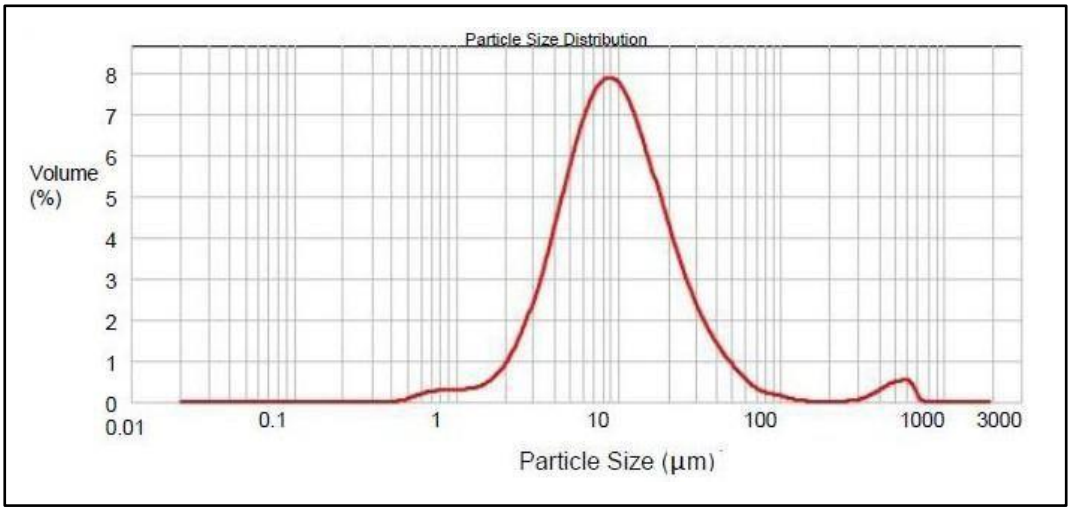

Fig. 4. Particle size distribution of Flutrimazole microsponges (Mean particle size 12.06µm).

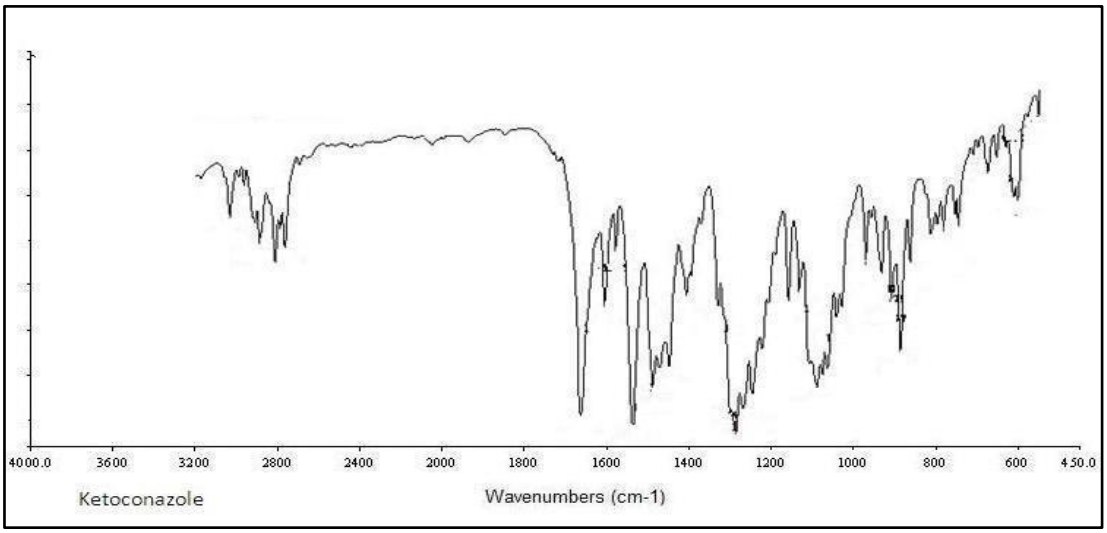

Fig. 5. FTIR Spectra of Flutrimazole.

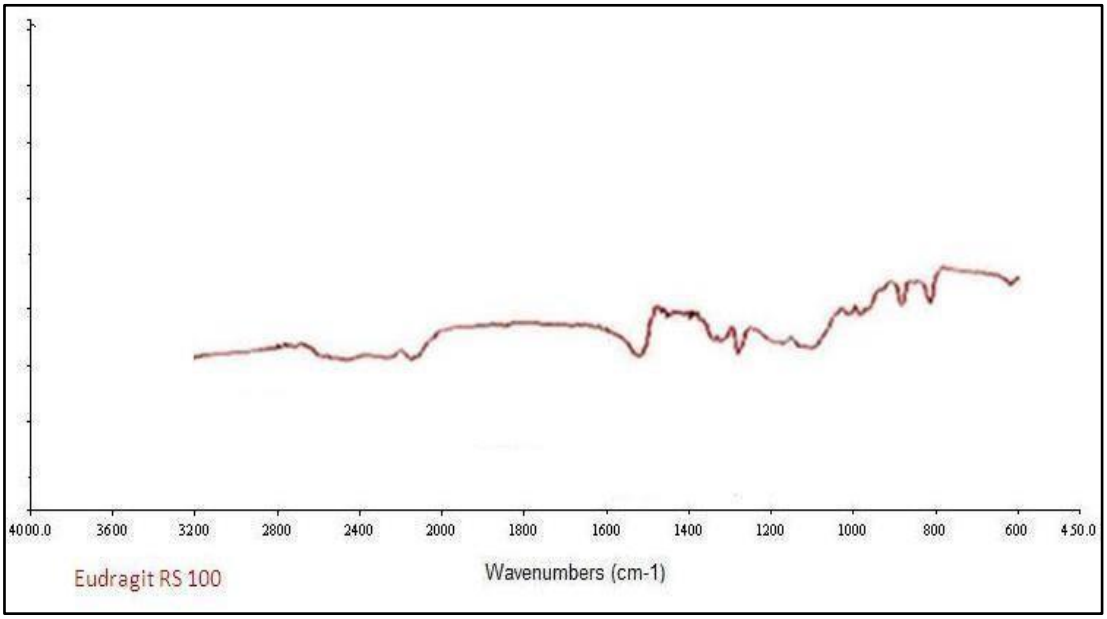

Fig. 6. FTIR Spectra of Eudragit RS100.

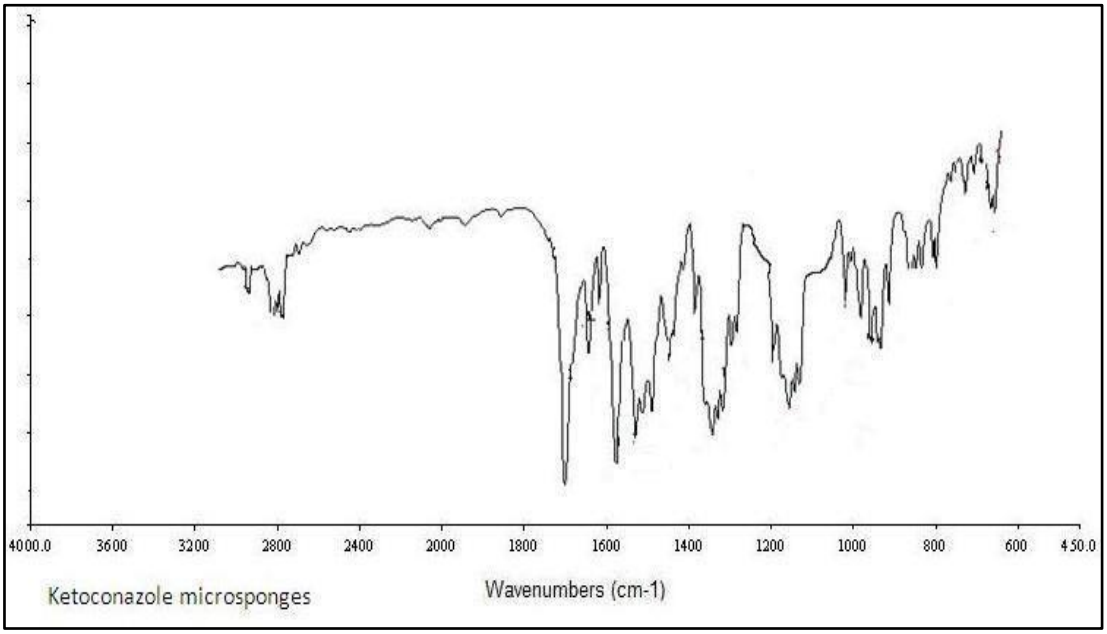

Fig. 7. FTIR Spectra of Eudragit microsponges containing Flutrimazole.

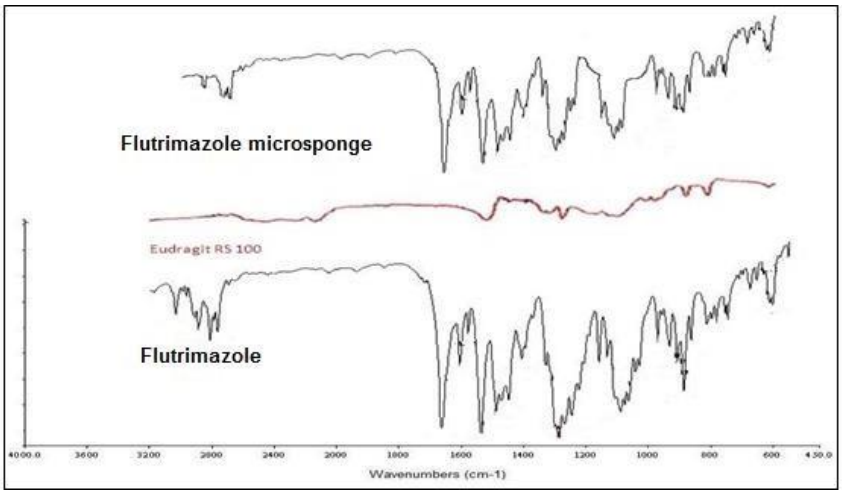

Fig. 8. Overlay FTIR Spectra of: Flutrimazole, Eudragit RS100 and Eudragit microsponges containing Flutrimazole.

The characteristic peaks of the medication in the infrared spectrum of F7 formulae were found to align with those of the corresponding unadulterated medications. Eudragit RS100 exhibited a peak corresponding to the stretching of the ester C=O bond. The findings indicated that no chemical interactions or alterations occurred throughout the preparation of the microsponge.

Differential Scanning Calorimetry (DSC)

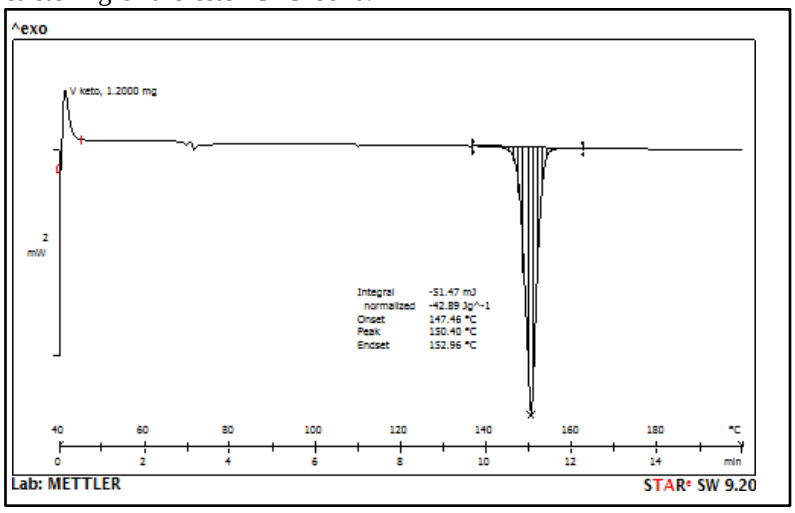

Fig. 9. DSC Thermogram of pure Flutrimazole.

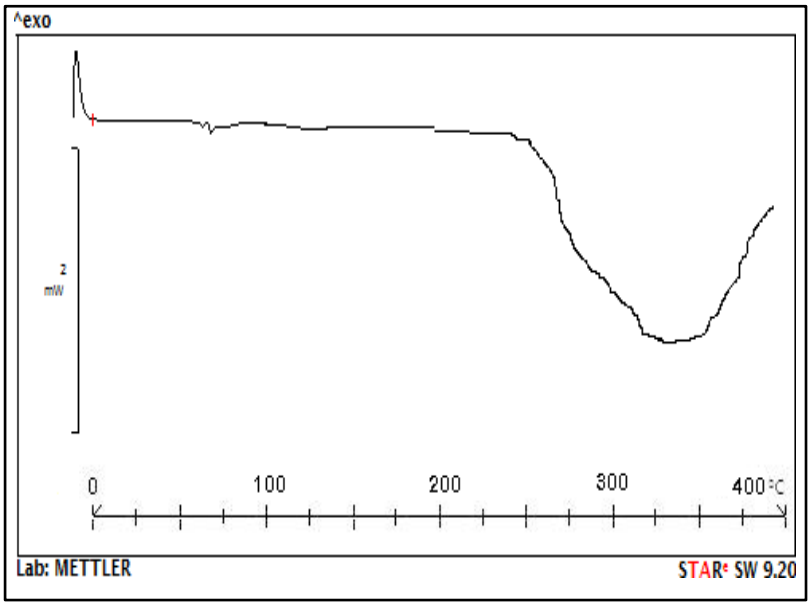

Fig. 10. DSC Thermogram of Eudragit RS 100.

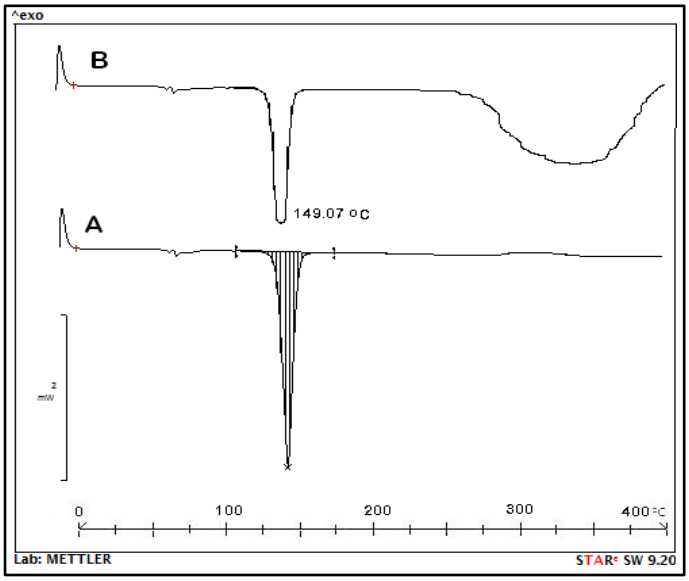

Fig. 11. Overlay DSC Thermograms of A:PureFlutrimazole, B:Eudragit microsponges containing Flutrimazole.

The DSC curves of the F7 preparations exhibited distinct peaks corresponding to Flutrimazole and Eudragit RS 100. The thermograms of the F7 version indicated an absence of interaction among the medication and the polymer.

Characterization of Pore Structure Mercury Intrusion Porosimetry (MIP). The volume of mercury intrusion is dependent on the overall porosity of the material. Fig. 12 illustrates the relationship between cumulative intrusion volume and the pressure applied, depicting the intrusion-extrusion profiles of selected microsponge preparations.

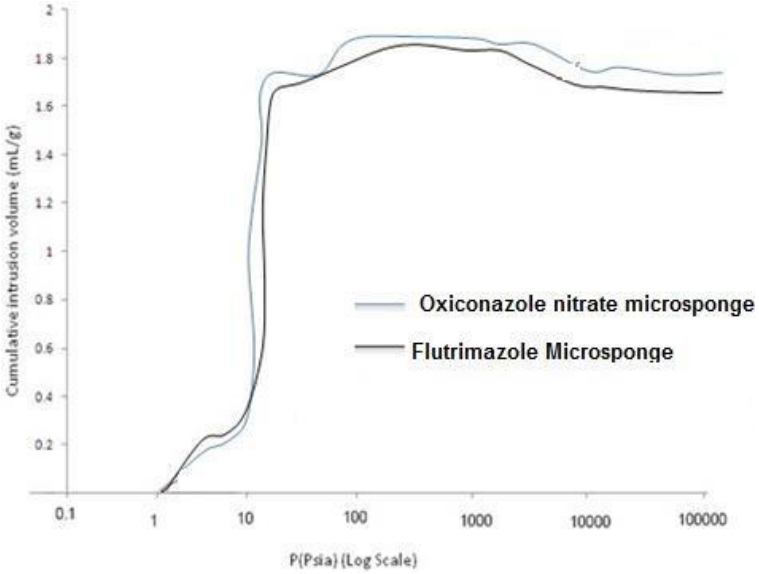

Fig. 12. Cumulative intrusion volume Vs Pressure curve of microsponge formulation.

As per intrusion plus extrusion curves, the majority of the pores present in Eudragit (Flutrimazole) microsponges were spherical type.

BET (Nitrogen adsorption) Method. BET multipoint adsorption isotherm studies, t-method micropore analysis and BJH desorption study was done by using nitrogen adsorption method[74] to find out external surface area, micro pore surface area (m^2/g), total pore volume and average pore diameter of representative Eudragit (Flutrimazole F7 microsponges). Table 8 shows values of BJH desorption plots of representative microsponges prepared by Eudragit method.

Table 8: External surface area, micro-pore surface area, total pore volume and average pore diameter of representative microsponge formulations (n= 3).

Formulation type	t-method external surface area(m^2/g)	t-method micro pore surface area(m^2/g)	Total pore volume (cc/g)	Average pore diameter (µm)
Flutrimazole Microsponges F7	5.37	4.27	1.63	0.26±0.06

*Each value is average of three separate determinations ±SD

***In-vitro* Release Study of Microsponge.** The drug release profiles of the Flutrimazole microsponge formulations are depicted in the accompanying table. The release of the drug from Flutrimazole microsponge exhibited a range between 68.32% and 77.25% across all formulations.

Table 9: In-vitro release study of Flutrimazole microsponges.

Time (Min)	Cumulative % drug release						
	F1	F2	F3	F4	F5	F6	F7
0	0	0	0	0	0	0	0
15	19.96±1.52	22.13±1.13	19.36±1.53	19.65±1.58	22.18±1.27	23.83±1.60	18.35±0.40
30	27.63±1.16	29.48±1.52	26.35±1.30	26.54±1.12	29.54±1.70	31.52±1.66	26.52±1.33
45	36.48±1.53	35.41±1.50	35.87±1.57	33.65±1.52	37.56±1.49	36.84±1.73	38.47±1.28
60	46.98±1.20	44.32±1.35	41.28±1.50	41.74±1.19	44.54±1.73	41.68±1.43	45.92±1.63
120	58.68±1.51	50.91±1.18	49.86±1.88	48.92±1.52	48.92±1.58	49.63±1.52	50.45±0.28
180	64.21±1.44	58.54±1.40	54.64±1.31	52.63±1.85	51.36±1.97	52.36±1.52	56.69±0.37
240	67.85±1.55	64.86±1.42	61.24±1.59	59.87±2.15	57.62±1.52	57.85±1.58	60.36±0.78
300	71.52±1.51	72.52±1.54	68.87±1.09	66.32±1.52	65.21±1.52	62.96±1.52	64.12±1.16
360	75.62±1.48	77.25±1.29	73.65±1.09	71.96±0.75	74.85±1.53	68.32±1.53	75.85±1.18

*****Each value is average of three separate

Stability Profile of Microsponge Formulation. The stability studies of the MDS formulation indicated that there were no notable alterations in the physical parameters when subjected to storage conditions of 40 ± 2°C and 75 ± 5% RH, thereby assessing their long-term stability. The samples were extracted and subsequently analyzed for drug content at intervals of 30 days, extending up to a duration of 6 months.

Table 10: Drug release profile of formulation F7 before and after stability.

Sampling Interval	Drug release (%) after 360 min*
	F7
0month	75.85±1.18
1month	74.56±0.36
2month	75.68±1.23
3month	75.235±1.65
4month	74.49±0.17
5month	75.28±1.59
6month	75.69±1.22

*****Each value is average of three separate determinations ±SD

The findings revealed that there was no notable decrease in the percentage of drug release over a span of 6 months; thus, no indications of drug degradation were detected.

Evaluation of gel loaded with microsponges and plain drug

Determination of Viscosity

Table 11: Viscosity of different gel formulations.

Gel formulation	Viscosity(cps)
Gel containing F7 microsponge	302478±1.21
Gel containing free Flutrimazole	232345±0.69

*****Each value is average of three separate determinations ±SD

The findings from the viscosity assessment of the gel indicate that the gel infused with microsponge exhibits a higher viscosity compared to the gel containing only the plain drug. The gels incorporating Eudragit microsponges infused with Flutrimazole exhibited a gritty texture.

Drug Diffusion from Microspongic Gels. Percentage of drug released from diffusion studies during 6 hrs. from gels containing free drug, drug entrapped in microsponges (F7) are shown in Table 12.

Table 12 : Cumulative %drug released from gels loaded with pure drug and microsponge entrapped drug.

Time in minute	Cumulative % drug released	
	Free Flutrimazole	F7
0	0	0
30	1.89±0.12	2.59±0.25
60	4.12±0.37	4.84±0.14
90	7.53±0.64	10.68±0.75
120	9.87±0.41	12.64±1.02
150	12.36±0.31	12.95±1.05
180	13.87±1.23	14.38±1.38
210	16.84±1.24	15.86±1.12
240	18.42±0.39	16.75±0.41
270	20.69±1.17	18.39±1.03
300	23.68±1.32	20.78±1.08
330	27.31±1.39	22.41±1.25
360	30.71±1.11	24.63±0.26

*****Each value is average of three separate determinations ±SD

The amount of drug diffused from gels containing free drugs and their respective drug entrapped microsponges i.e., F7 were found to be 32.44%, 30.71%, 31.59%. The controlled drug release was observed in all the microspongic gels. Drug release from all the microspongic gels were best fitted in Higuchi model (r^2= 0.978).

Table 13: Kinetic study for F7.

Sr. No.	Kinetic model	r^2
1.	First order	0.895
2.	**Higuchi**	**0.978**
3.	Korsemayer Peppas	0.969
4.	Hixon Crowell	0.970
5.	Zero order	0.963

CONCLUSIONS

The results highlight the potential of microsponge delivery systems for the topical administration of Flutrimazole, offering controlled release, reduced irritation, and potentially enhanced therapeutic outcomes.

FUTURE SCOPE

Overall, the developed microsponge system provides a novel and efficient topical drug delivery platform with

potential advantages such as reduced dosing frequency, improved patient compliance, and enhanced antifungal activity. The prepared formulation would be screened for Antifungal activity and Skin irritation toxicity.

Acknowledgement. The authors are thankful to Bhupal Nobles' University, Udaipur for providing the laboratory facilities.
Conflict of Interest. None

REFERENCES

Alomar, A., Videla, S., Delgadillo, J., Gich, I., Izquierdo, I., Forn, J. & Catalan Flutrimazole Study Group (1995). Flutrimazole 1% dermal cream in the treatment of dermatomycoses: a multicentre, double-blind, randomized, comparative clinical trial with bifonazole 1% cream: efficacy of flutrimazole 1% dermal cream in dermatomycoses. *Dermatology*, *190*(4), 295-300.

Aloorkar, N. H., Kulkarni, A. S., Ingale, D. J. & Patil, R. A. (2012). Microsponges as innovative drug delivery systems. *Int J Pharm Sci Nanotechnol*, *5*(1), 1597-1606.

Bargal, J. S., Dhawale, S. C., Landage, S. N. & Kulkarni, R. V. (2013). Formulation and evaluation of Eudragit RS 100 Loaded microsponges of Flutrimazole. *International Journal of Pharmaceutical Sciences and Research*, *4*(8), 3039.

Chen, H., Paul, S., Xu, H., Wang, K., Mahanthappa, M. K. & Sun, C. C. (2020). Reduction of punch-sticking propensity of celecoxib by spherical crystallization via polymer assisted quasi-emulsion solvent diffusion. *Molecular pharmaceutics*, *17*(4), 1387-1396.

Kaity, S., Maiti, S., Ghosh, A. K., Pal, D., Ghosh, A. & Banerjee, S. (2010). Microsponges: A novel strategy for drug delivery system. *Journal of advanced pharmaceutical technology & research*, *1*(3), 283-290.

Koparde, A., Shete, A., Patil, A., Mali, D., Durgawale, T., Yeligar, V. C., Shewale, M., Kadam, A. & Jadhav, R. (2023). Preparation and Characterisation of Silver Nanoparticles using Cissus Quadrangularis Extract and it's in vitro Anti-Arthritic Activity. *Biological Forum – An International Journal, 15*(3), 665-668.

Lengyel, M., Kállai-Szabó, N., Antal, V., Laki, A. J. &Antal, I. (2019). Microparticles, microspheres, and microcapsules for advanced drug delivery. *Scientia Pharmaceutica*, *87*(3), 20.

Lewis, R. E. (2011). Current concepts in antifungal pharmacology. In *Mayo Clinic Proceedings*, 86(8), 805-817. Elsevier.

Merlos, M., Vericat, M. L., Garcia-Rafanell, J. & Forn, J. (1996). Topical anti-inflammatory properties of flutrimazole, a new imidazole antifungal agent. *Inflammation Research*, *45*, 20-25.

Nafisi, S., &Maibach, H. I. (2018). Skin penetration of nanoparticles. In *Emerging nanotechnologies in immunology* (pp. 47-88). Elsevier.

Nevle, S. S. & Butle, S. R. (2023). Formulation Development and Evaluation of Taste-masked Moxifloxacin granules for the Treatment of Pediatric Tuberculosis. *Biological Forum – An International Journal, 15*(4), 450-455.

Prashanth, R., Kiran Kumar, A., Rajkumar, M. & Aparna, K. (2022). Studies on Postharvest Quality and Shelf Life of Pink Fleshed Dragon Fruit (Hylocereus spp.) Coated with Chitosan and Stored at Ambient Temperature. *Biological Forum – An International Journal*, *14*(3), 340-347.

Raina, N., Rani, R., Thakur, V. K. & Gupta, M. (2023). New insights in topical drug delivery for skin disorders: from a nanotechnological perspective. *ACS omega*, *8*(22), 19145-19167.

Ranade, V. V. (1991). Drug delivery systems. 6. Transdermal drug delivery. *The Journal of Clinical Pharmacology*, *31*(5), 401-418.

Singh Malik, D., Mital, N. & Kaur, G. (2016). Topical drug delivery systems: a patent review. *Expert opinion on therapeutic patents*, *26*(2), 213-228.

Syed, S. M., Gaikwad, S. S. & Wagh, S. (2020). Formulation and evaluation of gel containing fluconazole microsponges. *Asian Journal of Pharmaceutical Research and Development*, *8*(4), 231-239.

Thakur, S. & Desai, S. (2023). Formulation Development and Evaluation of Herbal Cream for Candidiasis. *Biological Forum – An International Journal, 15*(2), 01-08.

How to cite this article: Yogesh Kumar Garg and Amit Bhargava (2023). Formulation, Development and Characterization of Microsponges of Flutrimazole. *Biological Forum – An International Journal, 15*(6): 1035-1046.